COMMUNICATION

New Secrets of Spider Silk: Exceptionally High Thermal Conductivity and Its Abnormal Change under Stretching

Xiaopeng Huang, Guoqing Liu, and Xinwei Wang*

Generally, the thermal conductivity (k) of bulk polymers is very low[1] (on the order of 0.1 W m^{-1} K^{-1}) because of strong phonon scattering by various defects and interfaces.[2] In the past, various techniques have been attempted to increase the thermal conductivity of polymers via structure manipulation, like chain orientation improvement,[3,4] self-assembly of monolayers,[5] polyethylene chains alignment,[6] and ultra-drawing of polymer nanofibers.[7,8] Despite the low k of some tissues and organs,[9] the diversity of physical properties of carbon allotropes and amino-based proteins provides us with the confidence to seek a high-k biopolymer although the primary constituents of biomaterials are the same.

Spider silk has fascinated people for thousands of years due to its extraordinary combination of mechanical strength and elasticity that outperforms almost all synthetic materials.[10–12] It has inspired many studies aiming to unravel the mysterious mechanics.[10,13] According to a widely used kinetic model k $\sim \rho c_p v l = c_p l \sqrt{E \rho}$, the excellent Young's modulus E of spider dragline silk might lead to a high thermal conductivity (ρ: density, c_p: specific heat, v: sound speed, l: phonon mean free path). However, to date, the thermophysical properties of this potential great heat conductor have never been explored. Furthermore, it would be of great interest to explore the effect of strain on its thermophysical properties, which has not been investigated for other polymers, because spider silk displays extraordinary stretch abilities and supercontraction phenomenona (contracting by up to half in length)[14] caused by its unique hierarchical structure (**Figure 1**).[3,4,8] This exploration may also provide us with a clue about the protein structure configuration in spider silk fibers, which is still unclear.

We employed the generalized electrothermal (GET) technique[15] to measure the thermal properties of individual spider silk fibers and the effect of strain (see Experimental Section and Supporting Information). Spiders produce a family of different silks, some of which are strong and form structural parts of the web, while others are sticky and used to capture prey (Figure 1a). The benchmark dragline silk produced by the major ampullate gland of orb-weaver *Nephila clavipes* (*N. clavipes*)[16] is taken as the subject of our measurement. The schematic of the experimental setup is illustrated in **Figure 2**a including the stage specifically designed for measuring the thermal properties of silks under different strains. All the samples between the electrode

pairs (golden wires in Figure 2a) in one measurement were from the same individual silk fiber manually separated from a pair-silk thread. The sample-electrode contact is glued with silver paste (Figure 2b; 0.4 μm for average silver particle size) to make the thermal and electrical contact resistance negligible. The electrical contact resistance was confirmed to be negligible (~1 Ω) by an independent repetitive four-probe resistance measurement, compared with 5–8 kΩ for the coated film resistance in the thermal properties measurement. After finishing up the GET measurement, the diameters (~4 μm) of the samples were measured using scanning electron microscope (SEM, JEOL 5800LV, operated at 10 kV) at room temperature as shown in Figure 2b and c.

A typical normalized temperature evolution signal and corresponding fitting in the GET measurement is shown in **Figure 3**a. Very surprisingly, the measured thermal diffusivity α varies from $8.38 \pm 0.81 \times 10^{-5}$ to $12.30 \pm 1.18 \times 10^{-5}$ m^2/s (46.8% increase) and thermal conductivity k is from 348.7 ± 33.4 to 415.9 ± 33.0 W m^{-1} K^{-1} (19.3% increase) under strain ε from 3.9% to 19.7% (Figure 3b), respectively. Detailed results are in Table S1 and uncertainty calculation is in Supporting Information. The exceptionally high thermal conductivity we obtained is close to that of the second best metallic conductor: copper, and can be superior to copper after stretching the silk. We also clearly see that the thermal diffusivity and conductivity of the spider silk increase with strain and it does not show saturation, which indicates a potential large room for further enhancement. The thermal conductivity of the relaxed silk fiber (0% strain) can be extrapolated to be around 340 W m^{-1} K^{-1}. The increase trend at positive strains also makes spider silk a special material to tune up the thermal conductivity dynamically by stretching rather than compressing in general.[17] The comparison of thermophysical properties among several materials including supercontracted spider silk, another kind of silk, biotissues, a synthetic fiber, and a metal is represented in **Table 1**. The highest k of spider silk in our work (~416 W m^{-1} K^{-1}) is more than 800 times that of normal unperfused tissues (~0.5 W m^{-1} K^{-1}) and over 1000 times that of woven silkworm silk (~0.37 W m^{-1} K^{-1}). Both as natural materials, spider silk and tissues are close to the two extremes in thermal conductivity of condensed matter which only spans four orders of magnitude (~0.1–1000 W m^{-1} K^{-1}). In fact, the observed natural variability in mechanical properties of spider silk[16] also exists in the thermal properties. They depend on spider species, spiders (gender, age, health, and prey), silk environment, silk type and silk age. For the dragline silk, stretched or not, the measured k frequently lies in 150–300 W m^{-1} K^{-1}. The thermal diffusivity of spider silk can decrease by more than half (6.4 → 2.7 × 10^{-5} m^2 s^{-1}) after water-contraction with length decrease by ~24% and diameter increase by ~11% (4.734 → 4.237 μm).

Dr. X. Huang, G. Liu, Prof. X. Wang
Department of Mechanical Engineering
Iowa State University
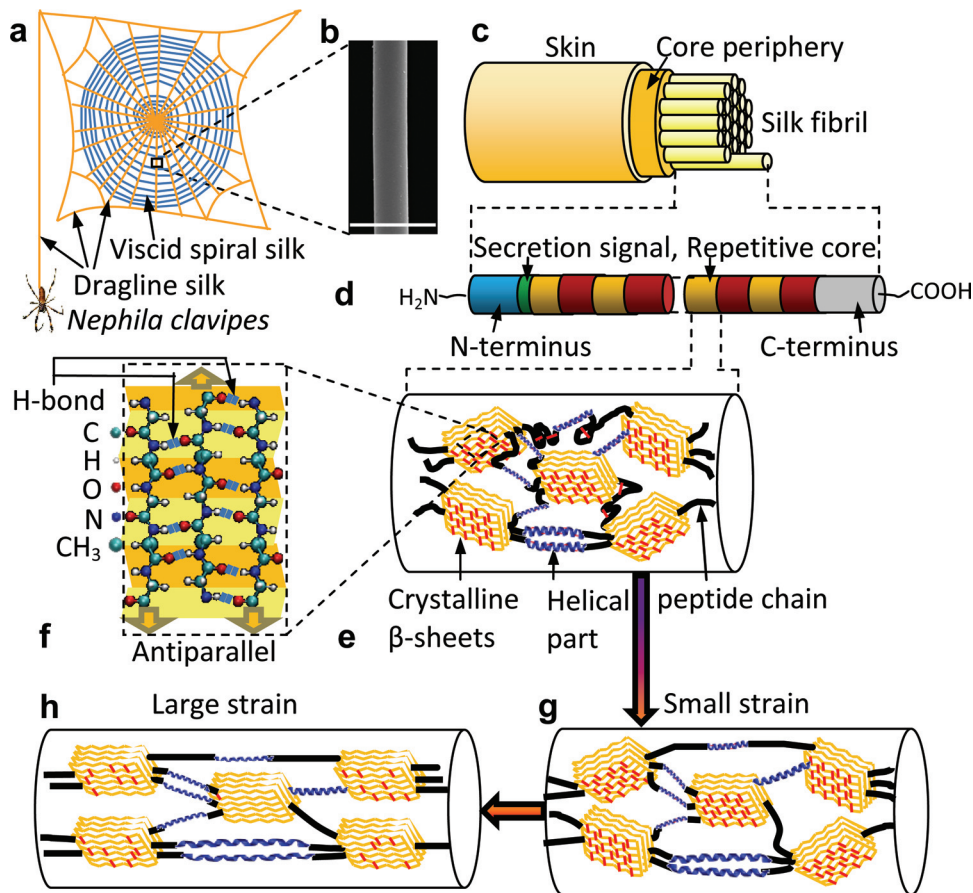Ames, IA 50011, USA
E-mail: xwang3@iastate.edu

Figure 1. a) A schematic orb-web built by a spider *N. clavipes*. b) A typical SEM image of an individual dragline silk. The scale bar is 10 μm. c) The skin-core structure of an individual dragline silk fiber. d) Compositions of a silk core fibril. e) The proteins contain highly oriented alanine-rich nanocrystals of antiparallel β-pleated sheets along the fiber axis embedded in a glycine-rich matrix of random polypeptide chains and moderately oriented helical structures. Short red lines between curves represent hydrogen bonds (H-bonds). f) The crystalline β-pleated sheets are made up of several antiparallel peptide chains. g) Under small strain, the intrachain H-bond breaking in the amorphous and moderately oriented domains is dominant. h) The inter-chain H-bond breaking in β-sheets and the stretching of covalent bonds along the protein backbone become dominant under large strains.

There will be a smaller decrease for k because both the specific heat and density will increase, especially for specific heat, due to increased hydrogen from the wetting. See Table S2 for details. Another fiber human hair, a kind of keratin protein like spider silk, has a measured thermal diffusivity of 4–5×10^{-7} m^2 s^{-1} (see Table S3), which is two orders of magnitude lower than that of spider silk. Note that the previous low k of silkworm silk was obtained in the out-of-plane direction of woven silks which should be dominated by the thermal contact resistance due to rough surface contact and the intrinsic inefficient phonon transport normal to the polypeptide chains. The k along the axial direction of single silkworm silks (~20 μm for effective diameter) can be one order of magnitude higher than that in perpendicular direction and normal tissues as shown in Table 1, and their α can be tripled at maximum under a middle strain ~65% (see Experimental Section and Supporting Information). Compared with spider dragline silk, the lower k and α of silkworm silk share the same reason with the lower strength. Another reason is likely the structure change induced by both thermal shrinkage and hydrogen loss during the baking process in preparation of dry silkworm silk (see Experimental Section).

According to $\alpha = k/\rho c_p$ and taking the reported value 1.36 g cm^{-3} for the density of *N. clavipes* dragline silk,[1] the specific heat c_p was calculated as 3061 ± 417 J kg^{-1} K^{-1} at 3.9% strain. As the strain increases to 19.7%, c_p decreases by about 24%, at 2487 ± 310 J kg^{-1} K^{-1}. Such a high volumetric specific heat (ρc_p) is larger than that of ammonia and close to that of water, benefiting a high k. The hydrogen loss in baked silkworm silk largely explains its much lower specific heat. From previous introduced $k \sim \rho c_p v l = c_p l \sqrt{E\rho}$ and assuming an averaged Young's modulus $E = 17$ GPa, the speed of sound v and effective phonon mean free path l in dragline silk can be estimated at around 3.5 km s^{-1} and 24–35 nm at strains 3.9%–19.7%.

The observed exceptionally high thermal conductivity of spider silk is largely attributed to its extraordinary structures, which are also responsible for its fantastic mechanical properties. At first, all naturally produced biomolecules, including proteins, are well-organized and less-defect structures associated with functionality formed by strong self-assembly.[18] Defect is a main source to reduce the strength and thermal conductivity in crystalline materials. The nanofibril (100 nm scale in diameter[19]) in *N. clavipes* silk fiber as shown in the
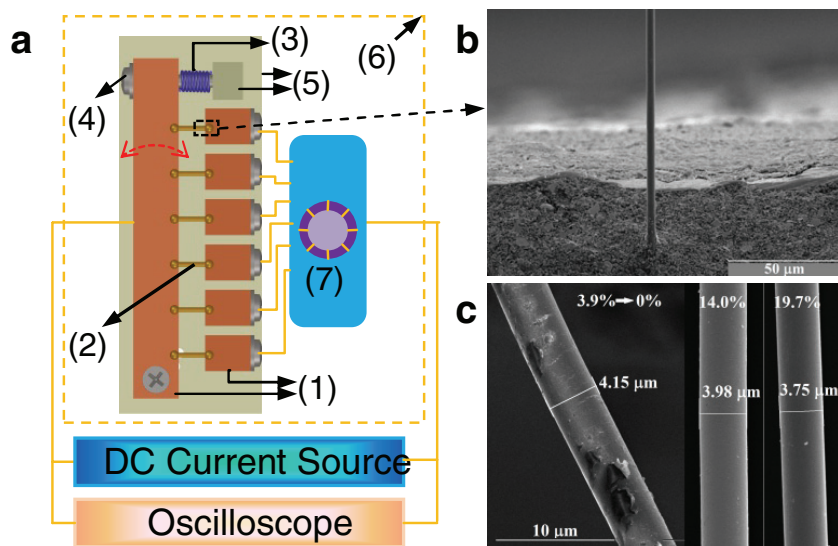
Figure 2. Schematic of the experimental system and SEM images of *N. clavipes* dragline silk. a) (1) Copper electrodes, (2) gold-coated sample, (3) compressed spring; (4) screw with the end in the (5) PVC block; (6) vacuum chamber; (7) switch for working on one sample per measurement. b) A typical mounting end of a spider silk fiber glued with silver paste. c) The three SEM images show that the silk fibers have uniform diameters. Note that the left-most 0% value indicates that a silk fiber which was originally stretched at 3.9% strain broke after finishing the calibration experiment.

a debate on the glycine-rich matrix (amorphous[19,20] or strongly oriented[21]), the crystalline β-pleated sheets made up of several antiparallel peptide chains (Figure 1f) should contribute much for efficient heat conduction like the theoretical prediction for single hydrocarbon chains[6], polyethylene chains,[7] and general oriented polymer fibers.[22] With their small fraction (~10%) in a spider silk, β-sheet crystals are expected to be able to have a much higher k than that of the hierarchically assembled silk according to the effective medium approximation. The high k results convinced us to believe the glycine-rich matrix has ordered structure that favors phonon energy transport. More importantly, we learned from the natural variability that the assembly pattern of nanostructures in biomaterials (at least silks) matters most for their macroscopic properties, no matter how similar the chemical composition and microscopic structures are (from spider to spider, or from spider to silkworm), not to mention the macrostructures (from spider silk to human hair). This is also true in carbon nanotube (CNT) applications (high k for individual CNT, low k for CNT bundles[15]).

The structure model of dragline silk can also help explain the enhancement effect of strain on the thermophysical properties observed in our measurements. The extensibility of spider silk is sacrificed by hydrogen bond (H-bond) network breaking (Figure 1e,h) and the strength lies on the stretching of covalent bonds along the protein backbone.[23] At small tensile strains, the intrachain H-bond breaking in the glycine-rich matrix is dominant and the alignment of noncrystals just has a small improvement since they are almost randomly distributed.
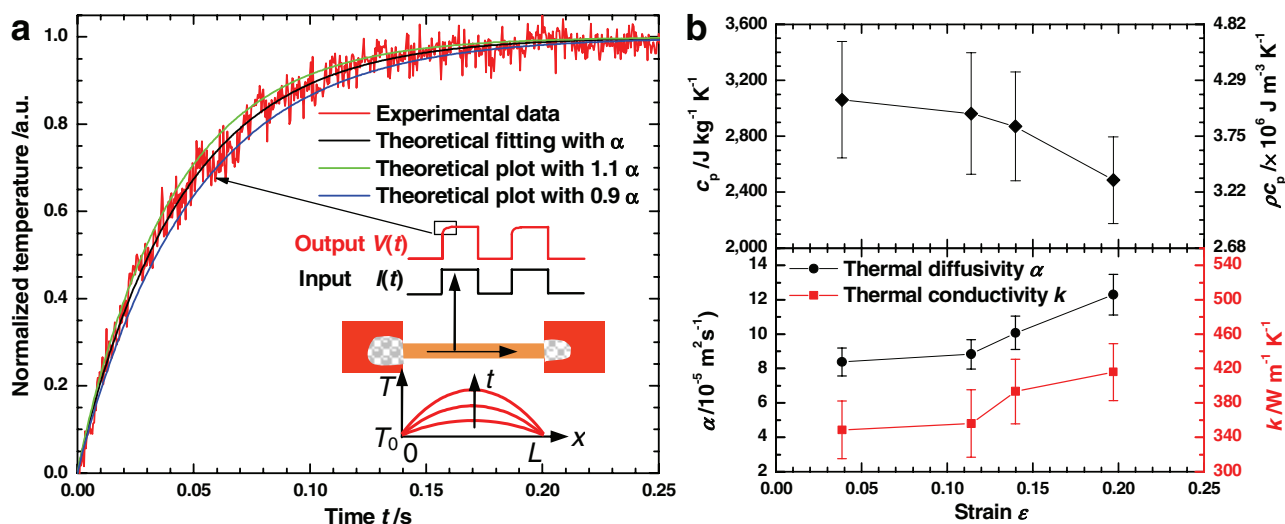
skin-core structures (Figure 1c), composed of two large repetitive proteins flanked by highly conserved non-repetitive amino-terminus (N-terminus) and carboxy-terminal (C-terminus)[11] (Figure 1d), have little defects. An unclear secretion signal is between N-terminus and repetitive proteins. More specifically, the proteins contain highly oriented alanine-rich nanocrystals of β-pleated sheets along the fiber axis embedded in a glycine-rich matrix of random polypeptide chains[19,20] and moderately oriented helical structures[21] (Figure 1e). Although there is

Figure 3. a) A typical curve fit forGET measurements. The lower inset is the schematic of the experimental setup including the sample stage, input/output signal, and a typical temperature profile history for a sample (Supporting Information). Theoretical curves with 1.1α and 0.9α are also plotted to illustrate the small uncertainty of the fit. b) The thermophysical properties of *N. clavipes* spider dragline silk under different strains.

Table 1. Comparison of properties among several materials (300 K).

Materials	α [10^{-5} m^2 s^{-1}]	k [W m^{-1} K^{-1}]	c_p [J kg^{-1} K^{-1}]	ρ [g cm^{-3}]	E [GPa]
NC dragline silk [a]	8.4, 12.3	349, 416	3060, 2490	1.36	12–22[1]
Silkworm silk ⊥ [b]	0.02 [c]	0.37[27]	1380[1]	1.35[1]	~10[1]
Silkworm silk ‖ [b]	0.17–0.40	2.4–4.7	874~1222		
Human hair	0.04–0.05			1.3	~9
Unperfused tissues[28]	~0.014	~0.5	700–4200	1–1.07	0–11.7
Kevlar 49	~1.4 [c]	~30	1480	1.44	124
Copper	11.23	401	385	8.94	110–128

[a]The two values are for the silk at the strain of 3.9% and 19.7%, respectively. *NC* represents *Nephila clavipes*; [b]‖ represents the values in the perpendicular direction of the woven silks and ‖ represents the values in the axis direction of slightly degummed single silks (α can be tripled after stretching). [c]Calculated by $\alpha = k/\rho c_p$.

Unsurprisingly, the enhancement of thermal diffusivity α and conductivity k is not large under small strains (Figure 3b). When the strain becomes large, the interchain H-bond breaking in crystalline β-pleated sheets and the stretching of covalent bonds along the protein backbone start to play the dominant role. The alignment of the inter- and intra- crystals are strongly enhanced,[20] which is attributed to straighter chains from lengthy curves between crystals and the smoothed polypeptide backbone from pleats in crystals.[19] Hence, α and k increase significantly at large strains (Figure 3b). The reduced phonon scattering due to H-bond breaking is also another factor for the k increase with strain. From the Raman spectra of an individual dragline silk from a *N. clavipes* web at different strains (Figure S1a, Supporting Information), the Raman wavenumber downshift was found for 1096 cm^{-1} (skeletal C$_\alpha$-C$_\beta$ stretching) and 1230 cm^{-1} (C-N stretching) peaks (Figure S1b, Supporting Information), which is consistent with the deformation of polymer fibers following a uniform stress series model.[24] The peak positions were determined after spectral decomposition (Figure S2, Supporting Information). The tensile strain decreases thermal conductivity in normal solid materials like silicon and diamond[17] due to the downward shift of phonon-dispersion curves under tensile strains which results in a smaller phonon group velocity. Therefore, our observed phenomenon for spider silk indicates a promising way for thermal transport tuning for soft materials with internal structures that will become more oriented under tensile strain. As for the specific heat, it is well known that more H-bonds lead to higher specific heat. Therefore, the specific heat has a larger decrease at large strains than at small ones (Figure 3b) because the broken intrachain H-bonds are much less than broken interchain H-bonds (Figure 1e, g, and h).

In summary, two new significant discoveries on the dragline silk of *N. clavipes* spider were reported. One is that the micrometer-size dragline silk has an exceptionally high thermal conductivity up to 416 W m^{-1} K^{-1} that beats most materials. The highly oriented antiparallel β-pleated sheets in silk fibrils

are expected to have a much higher thermal conductivity. The other is that the dragline silk has a surprising behavior contrary to normal solid materials: its thermal conductivity increases with strain significantly, up to 19% increase at ~20% strain. It opens a door for soft materials to be another option for thermal conductivity tuning. This enhancement effect is attributed to the intrachain and interchain H-bond breaking and improved crystal alignment under stretching. Our discoveries will revolutionize the conventional thought on the low thermal conductivity of biological materials.[9] Our results are expected to strongly stimulate innovations on the design paradigm of high-performance synthetic and gene-modified natural polymer fibers (e.g., silkworm silk) to improve their thermal conductivity in a revolutionary way. Polymers with superior thermal conductivity will find broader applications in flexible electronics, electronics packaging, and heat exchangers. Moreover, the biopolymers with high thermal conductivity may also have other potential application advantages because they are lightweight, tunable, biodegradable and electrically insulating.

Experimental Section

Sample preparation: Our spider silk filaments were produced by a mature *N. clavipes* female from Florida raised in the laboratory in 46 cm × 76 cm × 76 cm cages at 60%–70% relative humidity and a temperature of 23 °C. All the dragline samples were collected directly from the frame threads of a non-fresh-built web, which has no obvious difference for the Raman spectra (Figure 2a) compared with previous ones of web-harvested *N. clavipes* silks.[25] For the contracted silk sample, it was immersed in deionized water for 1 hour and then allowed to dry overnight in air. All silkworm silk samples were hand-reeled from *Bombyx mori* cocoons that were lightly degummed in boiling water for several minutes. They were then baked at 140 °C for 3 h for drying.

Thermal characterization: Gold sputter coating was performed on all samples with a film thickness around 25 nm. The stage with mounted samples was then placed in a vacuum chamber (1 mTorr). The evolution of voltage over the sample in the stimulus of a proper one-step DC current was recorded. Right after that, the temperature coefficient of resistance for the gold-coated spider silk was calibrated within 23–45 °C in the vacuum chamber. Please see Supporting Information for detailed procedures and results.

Raman characterization: Raman spectra were studied using a confocal Raman spectrometer (Voyage, BWTek, Inc, $\lambda = 532$ nm, 20 mW full power) coupled with an Olympus BX51 microscope. The beam was focused with 50× objective which gave a laser power about 8 mW on the sample. Combined with a caliper and a positioning stage, the beam point can be focused at almost the same place on the silk after stretching (Supporting Information). The spectra were obtained over the silk for an integration period of 20 s. Spectra were corrected for the fluorescence background over the 400–1800 cm^{-1} spectral region by subtracting a polynomial baseline. They were then smoothed by the Savitzky-Golay method with eight points. Wavenumber shifts due to experimental conditions of the spectrometer were corrected using the decomposited tyrosine band at 1615 cm^{-1} as in the literature.[26] For the spectral decomposition of 1615 cm^{-1} peak and interested peaks, a linear baseline was subtracted first and then the Lorentzian shape curve was used for the component peaks when doing fitting (Figure S2, Supporting Information).

Supporting Information

Supporting Information is available from the Wiley Online Library or from the author.

[1] *Polymer Data Handbook*, Oxford University Press, New York **1999**.

[2] H. G. Chae, S. Kumar, *Science* **2008**, *319*, 908.

[3] D. B. Mergenthaler, M. Pietralla, S. Roy, H. G. Kilian, *Macromolecules* **1992**, *25*, 3500.

[4] C. L. Choy, Y. W. Wong, G. W. Yang, T. Kanamoto, *J. Polym. Sci. Part B - Polym. Phys.* **1999**, *37*, 3359.

[5] R. Y. Wang, R. A. Segalman, A. Majumdar, *Appl. Phys. Lett.* **2006**, *89*, 173113.

[6] Z. Wang, J. A. Carter, A. Lagutchev, Y. K. Koh, N.-H. Seong, D. G. Cahill, D. D. Dlott, *Science* **2007**, *317*, 787.

[7] A. Henry, G. Chen, *Phys. Rev. Lett.* **2008**, *101*, 235502.

[8] S. Shen, A. Henry, J. Tong, R. Zheng, G. Chen, *Nat. Nanotechnol.* **2010**, *5*, 251.

[9] H. F. Bowman, E. G. Cravalho, M. Woods, *Annu. Rev. Biophys. Bioeng.* **1975**, *4*, 43.

[10] M. Xu, R. V. Lewis, *Proc. Natl. Acad. Sci. USA* **1990**, *87*, 7120.

[11] L. Romer, T. Scheibel, *Prion* **2008**, *2*, 154.

[12] Y. Yang, X. Chen, Z. Z. Shao, P. Zhou, D. Porter, D. P. Knight, F. Vollrath, *Adv. Mater.* **2005**, *17*, 84.

[13] a) N. Becker, E. Oroudjev, S. Mutz, J. P. Cleveland, P. K. Hansma, C. Y. Hayashi, D. E. Makarov, H. G. Hansma, *Nat. Mater.* **2003**, *2*, 278; b) F. Hagn, L. Eisoldt, J. G. Hardy, C. Vendrely, M. Coles, T. Scheibel, H. Kessler, *Nature* **2010**, *465*, 239.

[14] R. W. Work, *J. Arachnol.* **1981**, *9*, 299.

[15] X. Huang, J. Wang, G. Eres, X. Wang, *Carbon* **2011**, *49*, 1680.

[16] F. Vollrath, D. Porter, C. Holland, *Soft Matter* **2011**, *7*, 9595.

[17] X. Li, K. Maute, M. L. Dunn, R. Yang, *Phys. Rev. B* **2010**, *81*, 245318.

[18] C. Branden, J. Tooze, *Introduction to Protein Structure*, Garland Publishing Inc., New York **1999**.

[19] S. F. Y. Li, A. J. Mcghie, S. L. Tang, *Biophys. J.* **1994**, *66*, 1209.

[20] D. T. Grubb, L. W. Jelinski, *Macromolecules* **1997**, *30*, 2860.

[21] J. D. van Beek, S. Hess, F. Vollrath, B. H. Meier, *Proc. Natl. Acad. Sci. USA* **2002**, *99*, 10266.

[22] D. Porter, *Group itneraction Modelling of Polymer Properties*, Marcel Dekker, Inc., New York **1995**.

[23] A. Nova, S. Keten, N. M. Pugno, A. Redaelli, M. J. Buehler, *Nano Lett.* **2010**, *10*, 2626.

[24] W. Y. Yeh, R. J. Young, *Polymer* **1999**, *40*, 857.

[25] M. E. Rousseau, T. Lefevre, M. Pezolet, *Biomacromolecules* **2009**, *10*, 2945.

[26] T. Lefevre, M. E Rousseau, M. Pezolet, *Biophys. J.* **2007**, *92*, 2885.

[27] S. Baxter, F.N Surname, *Proc. Phys. Soc.* **1946**, *48*, 105.

[28] F. A. Duck, *Physical Properties of Tissue: a Comprehensive Reference Book*, Academic Press, London, **1990**.